

Effect of CeO_2 doping on the coercivity of 2:17 type SmCo magnets

Xiao-Lei Gao(高晓磊), Zhuang Liu(刘壮), Guang-Qing Wang(王广庆), Chao-Que Zhu(竺超群), Wen-Xin Cheng(程文鑫), Ming-Xiao Zhang(张明晓), Xin-Cai Liu(刘新才), Ren-Jie Chen(陈仁杰), and A-Ru Yan(闫阿儒)
Citation: Chin. Phys. B, 2023, 32 (**9**): 097504. DOI: 10.1088/1674-1056/acaa24
Journal homepage: http://cpb.iphy.ac.cn; http://iopscience.iop.org/cpb

What follows is a list of articles you may be interested in

Effect of TbF_3 diffusion on the demagnetization behavior and domain evolution of sintered Nd-Fe-B magnets by electrophoretic deposition

Xue-Jing Cao(曹学静), Shuai Guo(郭帅), Yu-Heng Xie(谢宇恒), Lei Jin(金磊), Guang-Fei Ding(丁广飞), Bo Zheng(郑波), Ren-Jie Chen(陈仁杰), and A-Ru Yan(闫阿儒)
Chin. Phys. B, 2023, 32 (**9**): 097503. DOI: 10.1088/1674-1056/acaf2d

Out-of-plane weak ferromagnetism at room temperaturein lattice-distortion non-collinear antiferromagnet of single-crystal Mn_3Sn

Bo-Xi Zhang(张博熙), Ping Song(宋平), Shan-Shan Deng(邓珊珊), Li Lou(娄理), and Sen Yao(姚森)
Chin. Phys. B, 2023, 32 (**8**): 087502. DOI: 10.1088/1674-1056/acca0b

Improvement of the microstructure and magnetic properties of (La,Ce)-Fe-B nanocrystalline ribbons

Li-Yu Lian(连李昱), Xiao-Wei Zhang(张晓伟), Ying Liu(刘颖), Jun Li(李军), and Ren-Quan Wang(王仁全)
Chin. Phys. B, 2023, 32 (**7**): 077501. DOI: 10.1088/1674-1056/acd8ae

Electric-field control of perpendicular magnetic anisotropy by resistive switching via electrochemical metallization

Yuan Yuan(袁源), Lu-Jun Wei(魏陆军), Yu Lu(卢羽), Ruo-Bai Liu(刘若柏), Tian-Yu Liu(刘天宇), Jia-Rui Chen(陈家瑞), Biao You(游彪), Wei Zhang(张维), Di Wu(吴镝), and Jun Du(杜军)
Chin. Phys. B, 2023, 32 (**6**): 067505. DOI: 10.1088/1674-1056/acbde8

Micromagnetic study of magnetization reversal in inhomogeneous permanent magnets

Zhi Yang(杨质), Yuanyuan Chen(陈源源), Weiqiang Liu(刘卫强), Yuqing Li(李玉卿), Liying Cong(丛利颖), Qiong Wu(吴琼), Hongguo Zhang(张红国), Qingmei Lu(路清梅), Dongtao Zhang(张东涛), and Ming Yue(岳明)
Chin. Phys. B, 2023, 32 (**4**): 047504. DOI: 10.1088/1674-1056/ac9359

Effect of CeO_2 doping on the coercivity of 2:17 type SmCo magnets

Xiao-Lei Gao(高晓磊)[1,2], Zhuang Liu(刘壮)[2,†], Guang-Qing Wang(王广庆)[2], Chao-Qun Zhu(竺超群)[1,2], Wen-Xin Cheng(程文鑫)[2], Ming-Xiao Zhang(张明晓)[2], Xin-Cai Liu(刘新才)[1,‡], Ren-Jie Chen(陈仁杰)[2], and A-Ru Yan(闫阿儒)[2]

[1] *School of Materials Science and Chemical Engineering, Ningbo University, Ningbo* 315211, *China*

[2] *CISRI & NIMTE Joint Innovation Center for Rare Earth Permanent Magnets, Ningbo Institute of Material Technology and Engineering, Chinese Academy of Sciences, Ningbo* 315201, *China*

(Received 19 July 2022; revised manuscript received 16 November 2022; accepted manuscript online 9 December 2022)

The effects of CeO_2 doping on the magnetic properties and microstructure of 2:17 type SmCo magnets are studied. With the increase of CeO_2 from 0 wt.% to 3 wt.%, the coercivity of the magnets increases from 22.22 kOe to over 29.37 kOe, which is an increase of more than 30%. When the doping content is lower than 1 wt.%, the remanence and magnetic energy product of the magnets remain almost constant. Both decrease sharply as the doping concentration further increases. After CeO_2 doping, the oxide content in the magnet increases significantly and the Ce element is uniformly distributed in the magnet. Observing the magnetic domains reveals that doping with CeO_2 can refine the magnetic domains and make the magnetic domain wall more stable, resulting in a significant increase in the coercivity of the magnets.

Keywords: 2:17 type SmCo magnets, coercivity, magnetic domain, microstructure

PACS: 75.50.Ww **DOI:** 10.1088/1674-1056/acaa24

1. Introduction

The 2:17 type SmCo magnets are known for their high Curie temperature, excellent thermal stability and good corrosion resistance. They are widely used in national defense, aerospace, rail transportation, instrumentation and other fields.[1–4] The coercivity is an important parameter of permanent magnet materials, which reflects their ability to resist demagnetization. For 2:17 type SmCo magnets, domain wall pinning has the greatest impact on the coercivity at room temperature.[5–7] Specifically, the pinning behavior of 2:17 type SmCo magnets is derived from the cellular structure consisting of an iron-rich intracellular phase ($Sm_2(Co,Fe)_{17}$, 2:17R), a Cu-rich cell boundary phase ($Sm(Co,Cu)_5$, 1:5H) and a Zr-rich layered phase ($(Sm,Zr)Co_3$).[8–11] Among them, the Cu-rich cell boundary phase is thought to play an important role in attracting or repelling pinning. Therefore, the Cu content in the cell boundary phase is the key factor for the high coercivity of the magnet.[12–15] Until now, the most effective method to change the coercivity of 2:17 type SmCo magnets has been to adjust and control the magnetocrystalline anisotropic field of the cell boundary phase.[16–18] In general, the magnetocrystalline anisotropy of the cellular structure can be effectively regulated by changing the content of Cu element that tends to be segregated in the cell boundary phase.[19,20]

The grain boundary of 2:17 type SmCo magnets is a Cu-lean region, resulting in an incomplete cellular structure around the grain boundary area, which destroys the pinning field and ultimately the coercivity.[21,22] To reduce the volume percentage of the Cu-lean region, one method is to increase the grain size of magnets,[23] but this method cannot eliminate the Cu-lean area near the grain boundary. Doping with Cu[24] and CuO[25] nanoparticles were found to reduce the Cu-lean region of 2:17 type SmCo magnets, by forming a complete cellular structure near the grain boundary, and improving the magnet's coercivity. This shows that the coercivity of 2:17 SmCo magnets can be effectively improved by changing the cellular structure near grain boundaries or phase boundaries.[25,26] Besides Cu and CuO, the coercivity of 2:17 type SmCo magnets can also be enhanced by doping with rare earth oxides. Wang *et al.*[27] reported that the coercivity increased from 20.24 kOe to 24.18 kOe by adding La_2O_3. The cellular structure near the $(La,Sm)_2O_3$ phase was found to grow larger in size, while the other cellular structure remained the same size as that in a magnet without doping. More importantly, the pinning field near the $(La,Sm)_2O_3$ phase was strengthened, which led to an increase in coercivity. La oxide can effectively improve the coercivity of magnets, and we suspect that Ce oxide also has the same effect.

In this work, the magnetic properties, microstructure, and magnetization behavior of 2:17 type SmCo magnets with added CeO_2 were studied in detail. Research results show that doping with CeO_2 can effectively improve the reverse demagnetization ability of the grain boundary region, and the size of the magnetic domain wall in the doped magnet is refined. This makes the domain wall energy more stable and improves the coercivity of the magnet.

[†]Corresponding author. E-mail: zliu@nimte.ac.cn

[‡]Corresponding author. E-mail: liuxincai@nbu.edu.cn

© 2023 Chinese Physical Society and IOP Publishing Ltd

2. Experiment

An alloy ingot with a nominal composition of $Sm(Co_{0.79}Fe_{0.09}Cu_{0.09}Zr_{0.03})_{7.68}$ was prepared in an induction melting furnace. An additional 1.5% Sm content was added to the alloy before melting, in order to compensate for the loss of the volatilization and oxide. Fine particles of about 3–4 μm in size were obtained after mechanical crushing and jet-milling. Commercially purchased CeO_2 particles are about 3 μm and their purity is more than 99.5%. The matrix powder was doped using 0 wt.%, 0.5 wt.%, 1 wt.%, 2 wt.%, and 3 wt.% of CeO_2 powder. The evenly mixed powders were pressed and oriented under a 2 T magnetic field to obtain the green body. After isostatic pressing, the green magnets were sintered at 1210 °C for 0.5 h for densification, followed by solution treatment at 1190 °C for 3 h. After 12 h of aging treatment at 830 °C, the magnets were cooled to 400 °C using a cooling rate of 0.7 °C/min and held at 400 °C for 4 h. Finally, the magnets were rapidly cooled to room temperature.

The magnetic properties of the magnet were measured using a BH tester (BH Nim-500C), and the maximum applied field was 8 T. The phase constitution was identified using an x-ray diffractometer (XRD) with a Philips diffractometer equipped with Cu $K\alpha$ radiation. The phase distribution was examined by a field emission scanning electron microscope (FE-SEM). The characterization of the microstructure was performed using a Tecnai F20 transmission electron microscope (TEM). The change in the magnetic domain was investigated using magneto-optical Kerr electron microscopy.

3. Results and discussion

Figure 1 shows the demagnetization curves and the variation curves of remanence (B_r), coercivity (H_{cj}) and maximum magnetic energy product $(BH)_{max}$ in $Sm(Co_{0.79}Fe_{0.09}Cu_{0.09}Zr_{0.03})_{7.68}$ magnets doped with different amounts of CeO_2. The coercivity increases greatly by doping with CeO_2. Based on the demagnetization curves in Fig. 1(a), the coercivity was 22.22 kOe for an undoped magnet, and it rose to 27.52 kOe after doping with 1 wt.% CeO_2. A further increase in the CeO_2 dopant amount to 2 wt.% increased the magnetic coercivity (to over 29.37 kOe). The B_r and $(BH)_{max}$ show a similar change trend with the adding of CeO_2. Both of them have an insignificant change when the doping amount of CeO_2 is $\leq$ 1 wt.%. In consequence, the B_r and $(BH)_{max}$ still maintain high values of 9.45 kGs and 21.7 MGOe for the 1 wt.% CeO_2 sample, respectively. However, these values decreased significantly to 9.07 kGs and 20.2 MGOe with further increase of the CeO_2 dopant to 3 wt.%, as shown in Fig. 1(b). This is because the density of the magnet decreases greatly with the increase of CeO_2. Moreover, the added CeO_2 is a non-magnetic substance, and its introduction will inevitably reduce the remanence.

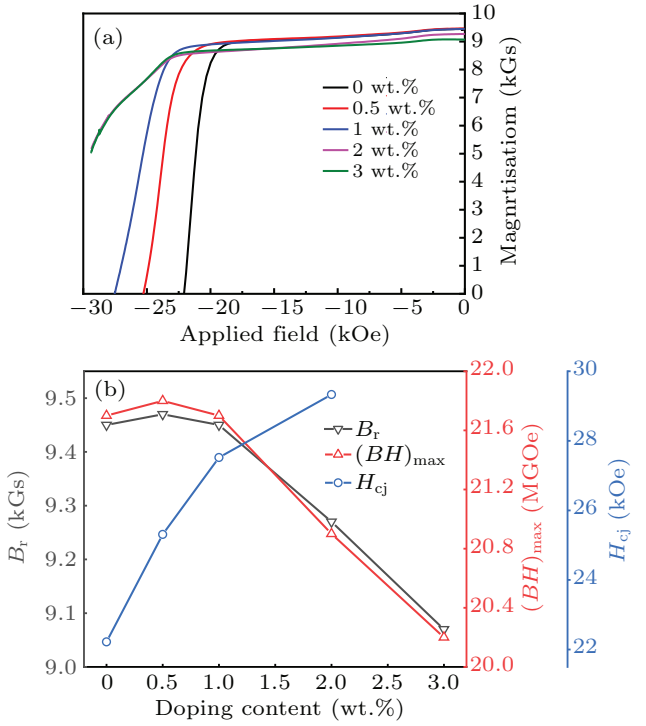


Fig. 1. Demagnetization curves (a) and the variation curves of remanence, coercivity and magnetic energy product (b) in $Sm(Co_{0.79}Fe_{0.09}Cu_{0.09}Zr_{0.03})_{7.68}$ magnets doped with different amounts of CeO_2.

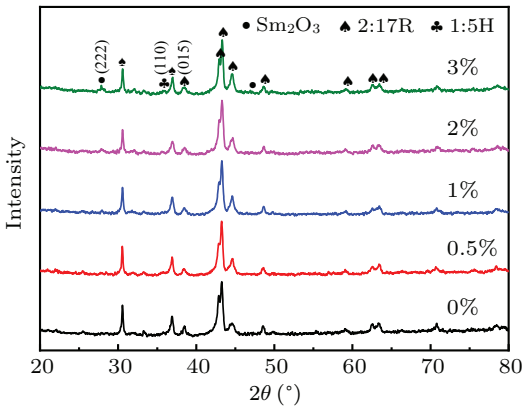


Fig. 2. XRD patterns of type 2:17 SmCo magnets with different CeO_2 contents in the aged state.

Figure 2 shows the x-ray diffraction of 2:17 type SmCo aged magnets doped with different amounts of CeO_2. It can be observed from the figure that the characteristic peak of the 2:17R phase – (015) peak was found to be near 38° for all the studied magnets. At this time, the main phase of the magnets with different CeO_2 contents was the 2:17R phase with a Th_2Zn_{17} type structure. This indicates that the magnet gradually evolved from a high temperature metastable disordered 1:7H phase in the solid solution state into a fully ordered 2:17R phase after a long period of aging treatment. In addition, the characteristic peak of the 1:5H phase – (110) peak was observed near 36° for these magnets, indicating the existence of a large number of Cu-rich cell wall phases with high magnetocrystalline anisotropic field. Here, diffraction peaks of the Zr-rich 1:3R flake phase are not found in the XRD pat-

tern because of the low overall content. In addition, Sm_2O_3, 2:17R, and 1:5H phases were observed in all the magnets, indicating that the main phase structure of the magnet was not affected by doping with CeO_2. In addition, the CeO_2 phase peak was not observed in the magnet with a CeO_2 doping content of 1 wt.%–3 wt.%. However, the peak intensity of the Sm_2O_3 phase shows an increasing trend. This could be a result of the replacement of the Ce element by the Sm element in the main phase, forming more of the samarium oxide phase, and the remaining cerium oxide may be too low to be detected.

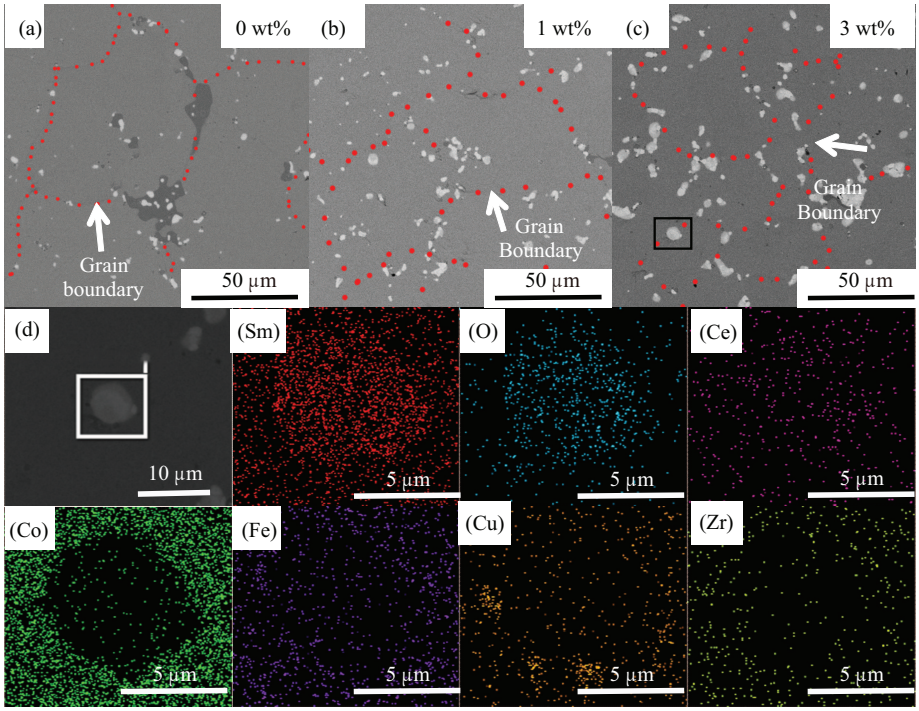


Fig. 3. (a)–(c) SEM images of CeO_2 doped magnets with different contents; (d) enlarged image of (c) and the corresponding element distribution.

Table 1. EDS dotting results of the gray matrix phase in aged magnets with different doping amounts.

CeO_2 (wt.%)	Sm (at.%)	Ce (at.%)	Co (at.%)	Fe (at.%)	Cu (at.%)	Zr (at.%)
0	12.42	0	68.52	10.50	7.31	1.25
0.5	10.73	0.18	69.01	10.29	8.26	1.53
1	10.83	0.20	68.93	10.99	7.61	1.44
2	9.85	0.41	70.38	10.43	7.16	1.77
3	10.68	0.59	68.48	11.01	7.69	1.55

Figures 3(a)–3(c) show the SEM images of magnets doped with 0 wt.%, 1 wt.%, and 3 wt.% CeO_2. In addition to the matrix phase (gray), all the aged magnets showed a certain amount of impure phases (white and black). According to the EDS results in Tables 1 and 2, the gray matrix phase is Fe-rich $Sm_2(Co,Fe)_{17}$, and the white phases are Sm-rich oxide. The black phase is found by calculation to be Zr-rich $Zr_6(Co,Fe)_{23}$ with Th_6Mn_{23} type structure. It can be seen that oxides mainly exist at grain boundaries. With the increase of the CeO_2 dopant, the amount of oxides in the sample increases gradually, while the $Zr_6(Co,Fe)_{23}$ phase decreases, and even disappeared when the amount of CeO_2 was higher than 3%, indicating the inhibiting effect of doping with CeO_2 on the formation of the black phase. Further analyzing the EDS results, one can find that increasing the CeO_2 dopant amount from 0 wt.% to 3 wt.% resulted in an increase in the percentage of Ce element in the matrix from 0 % to 0.59 %, and the atomic percentage of the Ce element in oxide gradually increases from 0 % to 1.57%. This shows that the Ce element can easily diffuse into the main phase within the doping amount of 3 wt.%. To study the distribution of the Ce element in the magnets, EDS mapping was performed on magnets with a doping amount of 3 wt.%, as shown in Fig. 3(d). The oxide is mainly enriched in Sm and O, while the matrix is mainly enriched in Sm, Co, and Fe, and the Ce element was evenly distributed in the matrix phase. The Ce element diffused into the main phase to replace the Sm element to form Ce_2Co_{17}. Due to the saturation magnetization of Ce_2Co_{17} being lower than that of Sm_2Co_{17}, the residual magnetization decreases.[28] The increase of coercivity is mainly due to the decrease of the Zr-rich impure phase. The Zr-rich impure phase deteriorates the coercivity of the magnets in two main aspects: (1) the Zr-rich heterogeneous phase, as a soft magnetic phase, can cause the adjacent grains to produce stray fields; and (2) the Zr-rich im-

pure phase consumes a large number of Zr atoms, resulting in a decrease in the contents of available Zr and Sm elements in the 2:17R intracellular phase and 1:5H cell wall phase, thus reducing the coercivity of the domain wall binding strength. With CeO_2 doping, the Ce element was uniformly distributed in the magnet, and reacted with the Fe and Co elements. As a result, the formation of the $Zr_6(Co,Fe)_{23}$ phase was inhibited and the coercivity of the magnet was improved.

Table 2. EDS dotting results of oxides in magnets with different doping levels.

CeO_2 (wt.%)	Sm (at.%)	Ce (at.%)	Co (at.%)	O (at.%)
0	55.87	0	7.30	36.83
0.5	52.96	0.30	6.20	40.54
1	54.65	0.63	2.82	41.90
2	58.44	0.84	2.27	38.45
3	49.04	1.57	1.34	48.05

The microstructure in the plane perpendicular to the *c*-axis for the 0 and 1 wt% CeO_2-doped samples is shown in Fig. 4. It can be seen from Fig. 4(a) that the undoped CeO_2 magnet has typical cell structure and continuous cell boundaries. The size range of the cell structure is about 90–100 nm, and the thickness of the cell wall is about 10 nm. In the sample doped with 1% CeO_2, the cell structure becomes more uneven and fine. The size range of the cell structure is about 35–80 nm, and the thickness of the cell wall is about 7 nm. Due to the decrease of cell structure and the increase of the cell wall phase, the coercivity of the magnet is improved.

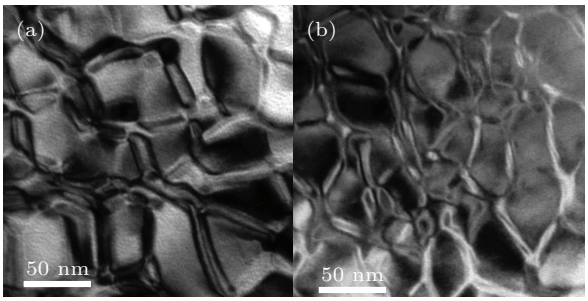


Fig. 4. TEM images of magnets with different CeO_2 contents; the plane of cellular structure perpendicular to the *c*-axis: (a) 0 wt.%, (b) 1wt.%.

To elucidate the enhancement mechanism of coercivity, we further studied the relationship between domain wall structure and applied magnetic field in doped magnets. Figure 5 shows the changes in magnetic domains during the magnetization of magnets doped with 0 wt.%, 1 wt.%, and 3 wt.% CeO_2. In the thermal demagnetization state, all the magnets show the strip magnetic domain structure within the grain. The direction of the strips is completely inconsistent between grains, resulting in a chaotic distribution of magnetic moments in the magnets. When the applied magnetic field is increased to 2.5 T, the observed steady narrowing of the white strip domains and the continual extension of the black domains in the undoped magnet indicate that the magnetic domain has been rotated by the applied field. The doped magnets showed insignificant change in the magnetic domain structure indicating that their magnetic moment pinning fields are stronger than that in the original magnet. When the field is increased to 3.5 T, the undoped magnet has been completely magnetized, and the chaotic magnetic domains inside the grains were not visible. In contrast, in the 1 wt.% CeO_2 doped magnet, there are no magnetic domains inside the grain, but a small number of domains with different directions were observed around the grain boundary. The 3 wt.% CeO_2 doped magnet showed a small number of domains with different directions inside the grain. There are still a small number of strip domains with different directions in the two doped magnets, indicating that the magnetization is not complete. When the applied magnetic field reaches 4 T, all three magnets are completely magnetized, no chaotic magnetic domains are observed inside the grains, and the domains in each grain are arranged in the same direction.

We also study the reverse magnetization of magnets. The magnet is magnetized with a magnetic field of 8 T to obtain a fully magnetized magnet, and then the magnetic field of the magnet is reduced to 0 T to obtain the remanent magnetic state magnet. The magnetic domains in each grain of the remanent magnet are aligned in the same direction. A reverse magnetic field is added to the remanent magnetic state magnet, and the magnet is demagnetized. Figure 6 shows the changes in magnetic domains during the reverse magnetization of 0 wt.%, 1 wt.%, and 3 wt.% CeO_2 with different doping. When a 2.5 T reverse magnetic field is applied to the magnet, the original magnet showed a reverse magnetic domain at the grain boundary (see the red arrow in Fig. 6), indicating that the magnet has been demagnetized around the grain boundary regions. It also means the pinning field is low for regions near the grain boundary in the original magnet. However, no reverse magnetic domain is observed in the doped magnet, indicating that the pinning ability of the domain wall has been strengthened around the grain boundary by doping with CeO_2. When the inverted magnetic field is increased to 3 T, the reverse magnetization of the original magnet takes place, and the white magnetic domain expands from the grain boundary into the grain (see the red arrow in Fig. 6). The reverse magnetization of the two doped magnets also occurs. The reverse white magnetic domain of the 1 wt.% CeO_2-doped magnets is also observed, spreading from the grain boundary to the interior of the grain. However, only some weak white reverse magnetic domain of the 3 wt.% CeO_2-doped magnets is observed at the grain boundary. When the applied reverse magnetic field reaches 3.5 T, the original magnets have been completely demagnetized, and the magnetic domains within the grains are aligned in the same direction. The reverse domain of the 1 wt.% CeO_2-doped magnet has completely spread into the grain, and the reverse domain of the 3 wt.% CeO_2-doped magnets has also started to spread into the grain.

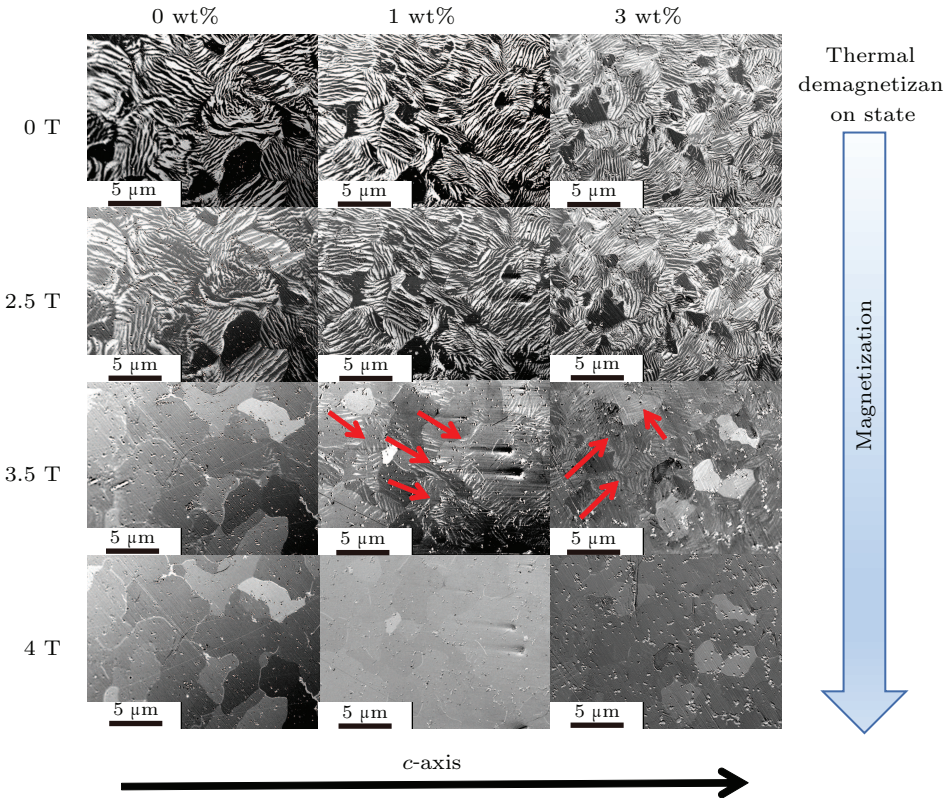


Fig. 5. Magnetic domain changes during magnetization for the magnets doped with 0 wt.%, 1 wt.%, and 3 wt.% CeO_2.

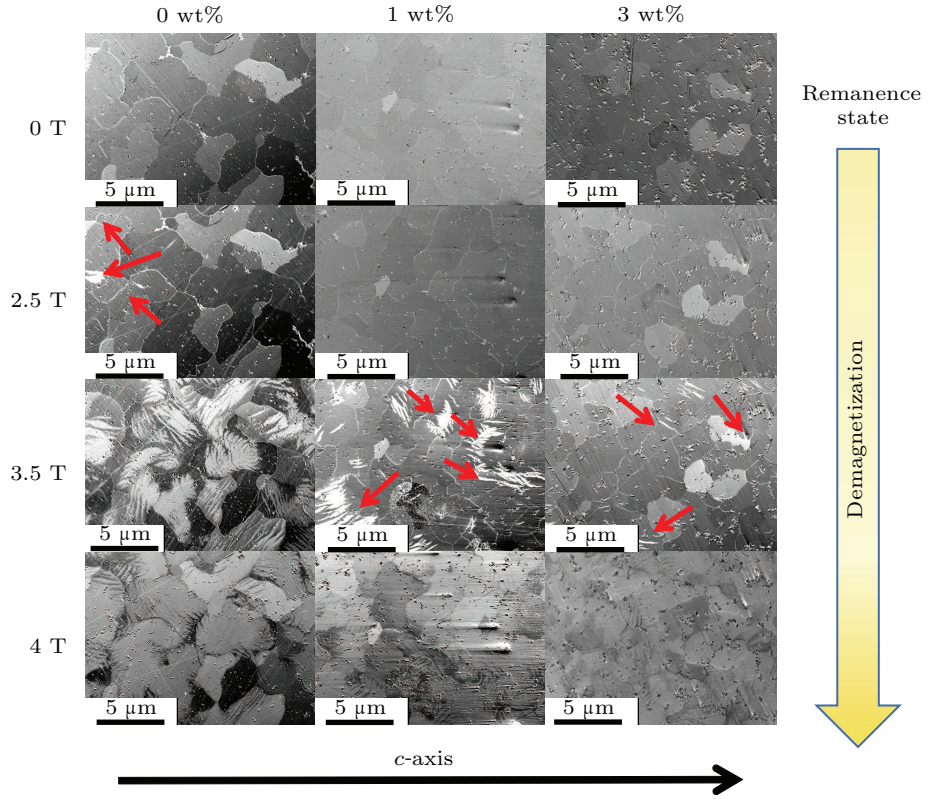


Fig. 6. Magnetic domain changes during reverse magnetization for the magnets doped with 0 wt.%, 1 wt.%, and 3 wt.% CeO_2.

The magnetization and reverse magnetization processes showed that the applied magnetic field required in the CeO_2-doped 2:17 type SmCo magnet is higher than that of the original magnet, meaning further improvement in coercivity for the doped magnet. More specifically, the magnetization inversion of both the original and doped magnets first occurs in the grain boundary region, and then propagates along the grain boundary to the interior of the grain. Thus, the pinning

field in regions around the grain boundary and grain interior are strengthened by doping with CeO_2, while the grain boundaries are still the weak pinning region. It can also be seen that the magnetic domain becomes thinner with the increase in CeO_2 doping amount. The finer the magnetic domain of the magnet, the higher the domain wall energy of the magnet, the higher the energy required for magnetization, and the higher the coercivity of the magnet.

4. Conclusion

A series of 2:17 type SmCo magnets containing Ce element and oxides were successfully prepared by the double-alloy method. The coercivity (H_{cj}) of magnets can be increased from 22.22 kOe to 27.52 kOe when adding 1 wt.% CeO_2, without reducing remanence and magnetic energy product. Further increasing the doping content to 3 wt.%, the H_{cj} exceeds 29.37 kOe, but B_r and $(BH)_{max}$ decrease obviously. The enhancement of coercivity for CeO_2-doped magnets originates from the improved pinning ability at the grain boundary and increased stability of the domain wall. A small amount of CeO_2 doping could be an effective way to obtain high-performance SmCo permanent magnets.

Data availability statement

The data that support the findings of this study are openly available in Science Data Bank at https://doi.org/10.57760/sciencedb.j00113.00097.

Acknowledgements

Project supported by the National Key R&D Program of China (Grant No. 2021YFB3503102), the Zhejiang Provincial Key R&D Program of China (Grant No. 2021C01191), and the Science and Technology Innovation 2025 Major Project of Ningbo (Grant No. 2020Z037).

References

[1] Jiang C, Venkatesan M, Gallagher K and Coey 2001 *J. Magn. Magn. Mater.* **236** 49
[2] Zhang C Y, Liu Z, Wang G Q, Yan G H, Chen R J, Lee D and Yan A R 2019 *J. Alloys Compd.* **795** 513
[3] Yang Q Q, Liu Z, Zhang C Y, Wu H C, Gao X L, Ma Y L, Chen R J and Yan A R 2021 *Chin. Phys. B* **30** 551
[4] Gutfleisch O, Willard M A, Ekkes Brück, Chen C H, Sankar S G and Liu J P 2011 *Adv. Mater.* **23** 821
[5] Goll D, Stadelmaier H H and Kronmüller H 2010 *Scr. Mater.* **63** 243
[6] Gutfleisch O, Müller K H, Khlopkov K, Wolf M, Yan A, Schäfer R, Gemming T and Schultz L 2006 *Acta Mater.* **54** 997
[7] Kronmüller H and Goll D 2002 *Scr. Mater.* **47** 545
[8] Sepehri-Amin H, Thielsch J, Fischbacher J, Ohkubo T, Schrefl T, Gutfleisch O and Hono K 2017 *Acta Mater.* **126** 1
[9] Xiong X Y and Finlayson T 2008 *J. Appl. Phys.* **104** 103910
[10] Duerrschnabel M, Yi M, Uestuener K, Liesegang M, Katter M, Kleebe H J and Molina-Luna L 2017 *Nat. Commun.* **8** 1
[11] Xue Z Q, Liu L, Liu Z, Li M, Lee D, Chen R J, Guo Y Q and Yan A R 2016 *Scr. Mater.* **113** 226
[12] Hadjipanayis G C, Tang W, Zhang Y, Chui S T, Liu J F, Chen C and Kronmüller H 2000 *IEEE Trans. Magn.* **36** 3382
[13] Liu S, Yang J, Doyle G, Potts G and Kuhl G E 2000 *J. Appl. Phys* **87** 6728
[14] Goll D, Stadelmaier H H and Kronmüller H 2010 *Scr. Mater.* **63** 243
[15] Kronmüller H and Goll D 2006 *J. Iron Steel Res. Int.* **13** 39
[16] Kronmüller H and Goll D 2008 *Phys. B* **403** 237
[17] Goll D, Kleinschroth I, Sigle W and Kronmüller H 2000 *Appl. Phys. Lett.* **76** 1054
[18] Liu J F, Chui T, Dimitrov D and Hadjipanayis G C 1998 *Appl. Phys. Lett.* **73** 3007
[19] Gopalan R, Hono K, Yan A and Gutfleisch O 2009 *Scr. Mater.* **60** 764
[20] Yan A, Bollero A, Müller K H and Gutfleisch O 2002 *Appl. Phys. Lett.* **80** 1243
[21] Horiuchi Y, Hagiwara M, Okamoto K, Kobayashi T, Endo M, Kobayashi T, Sanada N and Sakurada S 2014 *Mater.Trans.* **55** 482
[22] Horiuchi Y, Hagiwara M, Okamoto K, Kobayashi T, Endo M, Kobayashi T, Nakamura T and Sakurada S 2013 *IEEE Trans. Magn.* **49** 3221
[23] Wang Y Q, Yue M, Wu D, Zhang D T, Liu W Q, Zhang H G and Du Y H 2018 *J. Alloys Compd.* **741** 495
[24] Wang Y Q, Yue M, Wu D, Zhang D T, Liu W Q and Zhang 2018 *Scr. Mater.* **146** 231
[25] Yan G H, Liu Z, Xia W X, Zhang C Y, Wang G Q, Chen R J, Lee D, Liu P and Yan A R 2019 *J. Alloys Compd.* **785** 429
[26] Horiuchi Y, Hagiwara M, Endo M, Sanada N and Sakurada S 2015 *J. Appl. Phys.* **117** 1
[27] Wang G Q, Liu Z, Zhang C Y, Yang Q Q, Wu H C, Chen R J and Yan A R 2020 *J. Alloys Compd.* **849** 156589
[28] Senno H and Tawara Y 1974 *IEEE Trans. Magn.* **10** 313